JOURNAL OF SOLID STATE CHEMISTRY **136,** 79–86 (1998)
ARTICLE NO. SC977659

$K_4In_2(PSe_5)_2(P_2Se_6)$ and $Rb_3Sn(PSe_5)(P_2Se_6)$: One-Dimensional Compounds with Mixed Selenophosphate Anions

Konstantinos Chondroudis and Mercouri G. Kanatzidis[1]

Department of Chemistry, Michigan State University, East Lansing, Michigan, 48824

Received July 25, 1997; in revised form October 9, 1997; accepted October 10, 1997

The reaction of In with a molten mixture of $K_2Se/P_2Se_5/Se$ yielded brick-red, needle-like crystals of $K_4In_2(PSe_5)_2(P_2Se_6)$. The reaction of Sn with a molten mixture of $Rb_2Se/P_2Se_5/Se$ yielded black plate-like crystals of $Rb_3Sn(PSe_5)(P_2Se_6)$. Both compounds are stable in air and water. $K_4In_2(PSe_5)_2(P_2Se_6)$ crystallizes in the monoclinic space group *Cc* (9) with $a=11.1564(1)$ Å, $b=22.8771(1)$ Å, $c=12.6525(2)$ Å, $\beta=109.039(1)^\circ$, $Z=4$, and $R/R_w=4.1/4.4\%$. The one-dimensional structure features $[In_2(PSe_5)_2(P_2Se_6)]_n^{4n-}$ chains that consist of $In_2(PSe_5)_2$ dimers. These dimers are then bridged along the *a*-axis by tetradentate $[P_2Se_6]^{4-}$ units to form the chain. In^{3+} is in an octahedral environment. $Rb_3Sn(PSe_5)(P_2Se_6)$ crystallizes in the monoclinic space group $P2_1/a$ (14) with $a=14.013(2)$ Å, $b=7.3436(8)$ Å, $c=21.983(4)$ Å, $\beta=106.61(1)^\circ$, $Z=4$, and $R/R_w=3.5/4.4\%$. The one-dimensional structure features $[Sn(PSe_5)(P_2Se_6)]_n^{3n-}$ chains with octahedral Sn^{4+}. The neighboring Sn atoms are connected via tetradentate $[P_2Se_6]^{4-}$ units to form the chain. The $[PSe_5]^{3-}$ act as chelating side groups employing the diselenide "arm" and one of the monoselenide atoms to coordinate to Sn. The compounds were characterized with differential thermal analysis, far-IR, and solid-state UV/vis diffuse reflectance spectroscopy. © 1998 Academic Press

INTRODUCTION

Recent exploratory synthesis with the polychalcophosphate fluxes has yielded many novel quaternary thiophosphate and selenophosphate compounds (1). Many unusual compounds containing main group (2), transition metals (3), lanthanides, and actinides (2e, 2f, 4) have been reported. The basic building elements in these compounds are the negatively charged $[P_yQ_z]^{n-}$ (Q = S, Se) chalcophosphate units, which bind to the metal ions in an astonishing number of ways, forming extended covalent framework structures. The frameworks then incorporate alkali metal countercations according to their charge balancing needs. The great number of different $[P_yQ_z]^{n-}$ building blocks, along with their impressive bonding versatility, creates many possibilities for new structure types and compositions, most of which are unanticipated. The other important building block, the metal ion, also plays an important role in the stabilization of a specific structure, but this role is not fully understood yet. For example, in $K_3RuP_5Se_{10}$ we observe a protagonistic role for the metal (Ru) in determining ligand formation and selection according to its coordination chemistry needs (3e). Herein we report the synthesis, structural characterization, optical, and thermal properties of the new quaternary selenophosphate compounds $K_4In_2(PSe_5)_2(P_2Se_6)$ and $Rb_3Sn(PSe_5)(P_2Se_6)$.

[1] To whom correspondence should be addressed. E-mail: kanatzid@argus. cem.msu.edu.

EXPERIMENTAL SECTION

Reagents

The reagents mentioned in this study were used as obtained unless noted otherwise: (i) red phosphorus powder, Morton Thiokol, Inc., -100 mesh, Danvers, MA; (ii) rubidium metal, analytical reagent, Johnson Matthey/AESAR Group, Seabrook, NH; (iii) potassium metal, analytical reagent, Aldrich Chemical Co., Milwaukee, WI; (iv) selenium powder, 99.5 + % purity -100 mesh, Aldrich Chemical Co., Milwaukee, WI; (v) *N*,*N*-dimethylformamide (DMF) reagent grade, EM Science, Inc., Gibbstown, NJ; (vi) diethyl ether, ACS anhydrous, EM Science, Inc., Gibbstown, NJ.

Syntheses

A_2Se (A = K, Rb) were prepared by reacting stoichiometric amounts of the elements in liquid ammonia as described elsewhere (2).

The amorphous phosphorus selenide glass "P_2Se_5" was prepared by heating a stoichiometric ratio of the elements as described elsewhere (2).

Preparation of $K_4In_2(PSe_5)_2(P_2Se_6)$

A mixture of In (0.25 mmol), P_2Se_5 (0.5 mmol), K_2Se (0.5 mmol), and Se (2.5 mmol) was sealed under vacuum in

0022-4596/98 $25.00

a Pyrex tube and heated to 480°C for 3 days, followed by cooling to 150°C at 4°C h^{-1}. The excess $K_xP_ySe_z$ flux was removed by washing with DMF under N_2 atmosphere. The product was then washed with tri-*n*-butylphosphine to remove residual elemental Se and then ether to reveal analytically pure, brick-red needles (77% yield based on In). The crystals are air- and water-stable. Microprobe analysis carried out on several randomly selected crystals gave an average composition of $K_{1.7}InP_{1.9}Se_{8.2}$.

Preparation of $Rb_3Sn(PSe_5)(P_2Se_6)$

A mixture of Sn (0.3 mmol), P_2Se_5 (0.3 mmol), Rb_2Se (0.3 mmol), and Se (2.0 mmol) was sealed under vacuum in a Pyrex tube and heated to 495°C for 4 days followed by cooling to 150°C at 4°C h^{-1}. The flux was removed as above to reveal a mixture of black plates of $Rb_3Sn(PSe_5)$ (P_2Se_6) (70%) and black, irregular crystals of Rb_4Sn_5 $(P_2Se_6)_3Se_2$ (30%) (2e). The plate crystals were manually separated, and they are air- and water-stable. Microprobe analysis gave an average composition of $Rb_{2.8}SnP_{2.7}Se_{11.3}$.

Powder X-ray Diffraction (XRD)

Analyses were performed using a calibrated Rigaku-Denki/RW400F2 (Rotaflex) rotating anode powder diffractometer controlled by an IBM computer, operating at 45 kV/100 mA with a 1°/min. scan rate, employing Ni-filtered Cu radiation. Powder patterns were calculated with the CERIUS^2 software (5). Calculated and observed XRD patterns are deposited with the Supplementary Material.

Infrared Spectroscopy

Infrared spectra in the far-IR region (600–50 cm^{-1}) were recorded on a computer-controlled Nicolet 750 Magna-IR Series II spectrophotometer equipped with a TGS/PE detector and silicon beam splitter in 4 cm^{-1} resolution. The samples were ground with dry CsI into a fine powder and pressed into translucent pellets.

Solid State UV/Vis Spectroscopy

Optical diffuse reflectance measurements were performed at room temperature using a Shimadzu UV-3101PC double-beam, double-monochromator spectrophotometer. The instrument is equipped with integrating sphere and controlled by a personal computer. $BaSO_4$ was used as a 100% reflectance standard for all materials. Samples are prepared by grinding them to a fine powder and spreading them on a compacted surface of the powdered standard material, preloaded into a sample holder. The reflectance versus wavelength data generated can be used to estimate a material's band gap by converting reflectance to absorption data as described earlier (6).

Differential Thermal Analysis (DTA)

DTA experiments were performed on a computer-controlled Shimadzu DTA-50 thermal analyzer. Typically, a sample (~25 mg) of ground crystalline material was sealed in quartz ampoules under vacuum. A quartz ampoule of equal mass filled with Al_2O_3 was sealed and placed on the reference side of the detector. The samples were heated to the desired temperature at 10°C/min., then isothermed for 10 min., and finally cooled to 50°C at the same rate. Residues of the DTA experiments were examined by X-ray powder diffraction. To evaluate congruent melting, we compared the X-ray powder diffraction patterns before and after the DTA experiments. The stability and reproducibility of the samples were monitored by running multiple heating/cooling cycles.

Semiquantitative Microprobe Analyses

The analyses were performed using a JEOL JSM-6400V scanning electron microscope (SEM) with a TN 5500 EDS detector. Data acquisition was performed with an accelerating voltage of 20 kV and 30 s accumulation time.

Single Crystal X-ray Crystallography

Intensity data for $Rb_3Sn(PSe_5)(P_2Se_6)$ were collected using a Rigaku AFC6S four-circle automated diffractometer with a graphite crystal monochromator. Crystal stability was monitored with three standard reflections whose intensities were checked every 150 reflections, and no crystal decay was detected. An empirical absorption correction based on ψ scans was applied to all data during initial stages of refinement. An empirical DIFABS correction was applied after full isotropic refinement, as recommended (7), after which full anisotropic refinement was performed. A Siemens SMART Platform CCD diffractometer was used to collect data for $K_4In_2(PSe_5)_2(P_2Se_6)$. An empirical absorption correction (8) was applied to the data. The space groups were determined from systematic absences and intensity statistics. To check for the correct enantiomorph for K_4In_2 $(PSe_5)_2(P_2Se_6)$, we refined the Flack parameter, which yielded the value of 0.0. Attempts at the other two possible space groups, $C2/c$ and $C2$, were unsuccessful. The structures were solved by direct methods using SHELXS-86 software (9a), and full-matrix least-squares refinement was performed using the TEXSAN software package (9b).

The complete data collection parameters and details of the structure solution and refinement are given in Table 1. The coordinates of all atoms, average temperature factors, and their estimated standard deviations are given in Tables 2 and 3.

RESULTS AND DISCUSSION

Description of Structures

The structure of $K_4In_2(PSe_5)_2(P_2Se_6)$ is shown in Fig. 1. The compound has one-dimensional infinite chains of $[In_2(PSe_5)_2(P_2Se_6)]_n^{4n-}$ that contain $In_2(PSe_5)_2$ dimers. Each dimer is formed by two edge-sharing $InSe_6$ octahedra that are bridged via tridentate $[PSe_5]^{3-}$ ligands (Fig. 1b). Every $[PSe_5]^{3-}$ ligand employs two monoselenides to coordinate to the In atoms [e.g., Se(7), Se(9)] and one Se atom from the diselenide "arm" that is shared by both In atoms [e.g., Se(11)]. Two such ligands cap the dimer from above and below, yielding an In–In distance of 4.036(2) Å. The dimers are then linked along the *a*-axis by tetradentate $[P_2Se_6]^{4-}$ ligands to form the chain. The $[P_2Se_6]^{4-}$ unit adopts the staggered conformation and employs two Se atoms from each P [e.g., Se(1), Se(2) from P(1)] to bridge the neighboring dimers, while the third Se is noncoordinating. A similar chain structure exists in $K_2MP_2S_7$ ($M = V, Cr$), which contain $[M_2(PS_4)_2(P_2S_6)]_n^{4n-}$ chains (10). In these chains $M_2(PS_4)_2$ dimers are linked by tetradentate $[P_2S_6]^{4-}$ ligands in a different coordination mode than those of

TABLE 1
Crystallographic Data for $K_4In_2(PSe_5)_2(P_2Se_6)$ and $Rb_3Sn(PSe_5)(P_2Se_6)$

Formula	$K_4In_2P_4Se_{16}$	$Rb_3SnP_3Se_{11}$
FW	1773.29	1336.57
a, Å	11.1564(1)	14.013(2)
b, Å	22.8771(1)	7.3436(8)
c, Å	12.6525(2)	21.983(4)
α (deg)	90.00	90.00
β (deg)	109.039(1)	106.61(1)
γ (deg)	90.00	90.00
Z, *V* (Å^3)	4; 3052.60(5)	4; 2167.7(6)
λ (Mo$K\alpha$), Å	0.71073	0.71069
Space group	*Cc* (No. 9)	$P2_1/a$ (No. 14)
D_{calc}, g/cm^3	3.858	4.095
μ, cm^{-1}	213.44	261.92
Temp (°C)	20	23
Final R/R_w,[a] %	4.1/4.4	3.5/4.4
Total data measured	13355	3485
Total unique data (avg.)	5357	3305
Data $F_o^2 > 3\sigma(F_o^2)$	2190	1993
No. of variables	235	163
Crystal dimen. (mm)	$0.50 \times 0.15 \times 0.15$	$0.28 \times 0.12 \times 0.04$

[a] $R = \sum(|F_o| - |F_c|)/\sum|F_o|$; $R_w = \{\sum_w(|F_o| - |F_c|)^2/\sum_w|F_o|^2\}^{1/2}$

TABLE 2
Positional Parameters and *B*(eq)[a] for $K_4In_2(PSe_5)_2(P_2Se_6)$

Atom	*X*	*Y*	*Z*	B_{eq}[a] (Å^2)
In(1)	0.3819(2)	0.11792(6)	0.6830(1)	1.76(3)
In(2)	0.7462(2)	0.12163(5)	0.6906(1)	1.63(3)
K(1)	0.8435(5)	0.1993(2)	0.3490(4)	3.9(1)
K(2)	0.8152(4)	0.0615(2)	0.0701(4)	3.1(1)
K(3)	0.4083(4)	0.1972(2)	0.3234(4)	3.3(1)
K(4)	0.2044(4)	0.0550(2)	1.0171(4)	3.3(1)
P(1)	0.0874(4)	0.1626(2)	0.7426(4)	1.19(9)
P(2)	0.0469(4)	0.0827(2)	0.6333(4)	1.22(9)
P(3)	0.5613(5)	0.2657(2)	0.6709(4)	1.58(10)
P(4)	0.5737(5)	−0.0254(2)	0.7058(4)	1.66(10)
Se(1)	0.2852(2)	0.15112(8)	0.8486(2)	1.62(4)
Se(2)	0.9671(2)	0.15123(8)	0.8525(2)	1.63(4)
Se(3)	0.0466(2)	0.23919(7)	0.6406(2)	2.00(4)
Se(4)	0.0877(2)	0.00594(8)	0.7349(2)	1.98(4)
Se(5)	0.8423(2)	0.09023(8)	0.5293(2)	1.57(4)
Se(6)	0.1547(2)	0.09720(8)	0.5185(2)	1.71(4)
Se(7)	0.3669(2)	0.23119(8)	0.5961(2)	2.15(4)
Se(8)	1.0715(2)	0.14018(8)	1.1880(2)	2.38(4)
Se(9)	0.6975(2)	0.23106(8)	0.5960(2)	2.07(4)
Se(10)	0.6240(2)	0.24433(8)	0.8539(2)	1.91(4)
Se(11)	0.6200(2)	0.14238(8)	0.8443(2)	1.57(4)
Se(12)	0.5081(2)	0.09500(8)	0.5301(2)	1.55(4)
Se(13)	0.5146(2)	−0.00709(8)	0.5202(2)	1.67(4)
Se(14)	0.4094(2)	0.00407(8)	0.7548(2)	1.86(4)
Se(15)	0.58010(2)	0.11975(8)	0.1986(2)	2.57(4)
Se(16)	0.7599(2)	0.01333(8)	0.7878(2)	1.85(4)

[a] *B* values for anisotropically refined atoms are given in the form of the isotropic equivalent displacement parameter defined as $B_{eq} = \frac{4}{3}[a^2B(1,1) + b^2B(2,2) + c^2B(3,3) + ab(\cos\gamma)B(1,2) + ac(\cos\beta)B(1,3) + bc(\cos\alpha)B(2,3)]$

TABLE 3
Positional Parameters and *B*(eq)[a] for $Rb_3Sn(PSe_5)(P_2Se_6)$

Atom	*X*	*Y*	*Z*	B_{eq}[a] (Å^2)
Sn	0.22167(6)	0.6390(1)	0.27946(5)	1.52(4)
Rb(1)	0.3880(1)	0.6712(2)	0.51104(9)	3.07(7)
Rb(2)	0.0128(1)	1.1318(2)	0.2296(1)	3.32(8)
Rb(3)	0.3451(1)	0.9667(3)	0.07028(9)	3.79(8)
Se(1)	0.2390(1)	0.3466(2)	0.21400(8)	2.06(6)
Se(2)	0.3268(1)	0.4647(2)	0.08140(9)	3.01(8)
Se(3)	0.0768(1)	1.2698(2)	0.05704(9)	3.29(8)
Se(4)	0.1152(1)	0.7123(2)	0.10986(8)	2.32(6)
Se(5)	0.2259(1)	0.8773(2)	0.19115(8)	2.34(7)
Se(6)	0.2040(1)	0.8801(2)	0.36949(8)	1.89(6)
Se(7)	0.2036(1)	0.4001(2)	0.37357(8)	1.82(6)
Se(8)	0.1178(1)	0.6527(2)	0.49267(7)	2.14(6)
Se(9)	0.0144(1)	0.6328(2)	0.23323(7)	1.89(6)
Se(10)	0.4180(1)	0.6054(2)	0.34440(8)	1.91(6)
Se(11)	0.4011(1)	1.1083(2)	0.34219(8)	2.48(7)
P(1)	0.1941(3)	0.4382(5)	0.1124(2)	2.0(2)
P(2)	0.1280(2)	0.6433(5)	0.3977(2)	1.5(1)
P(3)	−0.0210(2)	0.6274(5)	0.3260(2)	1.5(1)

[a] *B* values for anisotropically refined atoms are given in the form of the isotropic equivalent displacement parameter defined as $B_{eq} = \frac{4}{3}[a^2B(1,1) + b^2B(2,2) + c^2B(3,3) + ab(\cos\gamma)B(1,2) + ac(\cos\beta)B(1,3) + bc(\cos\alpha)B(2,3)]$

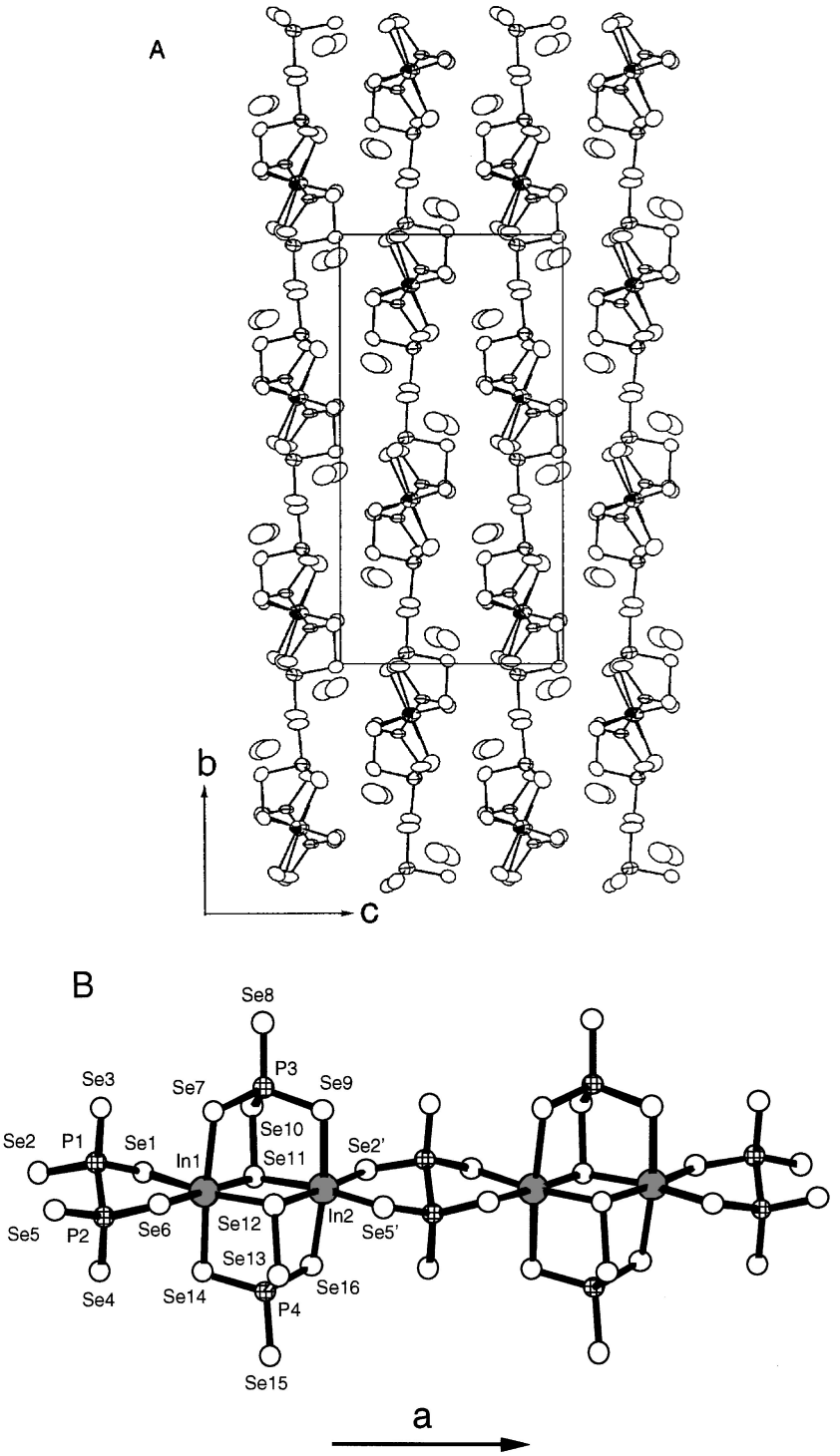

FIG. 1. (A) Unit cell of $K_4In_2(PSe_5)_2(P_2Se_6)$ viewed down the *a*-axis. In the infinite part of the structure, indium is shown as octant shaded ellipses, selenium as open ellipses, and phosphorus as crossed ellipses. The K^+ ions located between the chains are shown as open ellipses. (B) An isolated $[In_2(PSe_5)_2(P_2Se_6)]_n^{4n-}$ chain with labeling.

$K_4In_2(PSe_5)_2(P_2Se_6)$. For comparison, the repeating units of the $K_4In_2(PSe_5)_2(P_2Se_6)$ and $K_2MP_2S_7$ are shown in Scheme 1A and 1B, respectively.

In $K_4In_2(PSe_5)_2(P_2Se_6)$, there are two sets of In–Se distances: the first set of long distances averages 2.80(2) Å, and the second set of short distances averages at 2.74(2) Å.

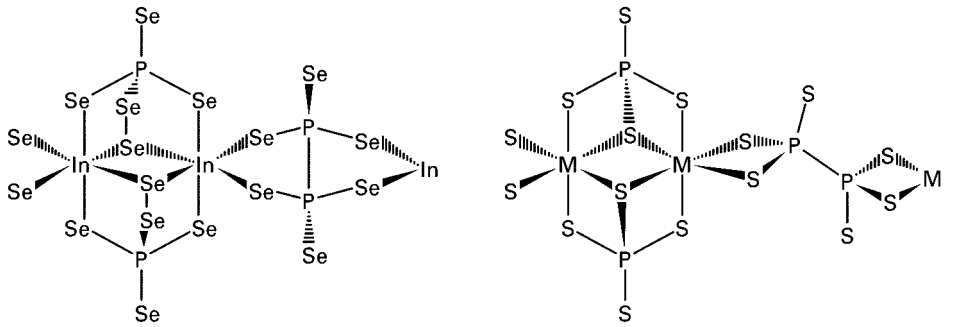

SCHEME 1

Similar distances have been observed in $In_4(P_2Se_6)_3$ (11). The $[In_2(PSe_5)_2(P_2Se_6)]_n^{4n-}$ chains are separated by K^+ ions located in four different sites. K(1) is coordinated by seven Se atoms [range of K(1)–Se distances, 3.367(6)–3.769(7) Å, avg. 3.552 Å], K(2) is eight-coordinated [3.295(6)–3.744(7) Å, avg. 3.502 Å], K(3) is eight-coordinated [3.366(6)–3.815(6) Å, avg. 3.546 Å], and K(4) is also eight-coordinated [3.384(6)–3.685(6) Å, avg. 3.538 Å]. Selected distances and angles for $K_4In_2(PSe_5)_2(P_2Se_6)$ are given in Table 4.

The structure of $Rb_3Sn(PSe_5)(P_2Se_6)$ is shown in Fig. 2. The compound features one-dimensional infinite chains of $[Sn(PSe_5)(P_2Se_6)]_n^{3n-}$ consisting of $Sn(PSe_5)$ units stacked parallel to the *a* axis. The $[PSe_5]^{3-}$ ligands are bidentate and use one monoselenide and the diselenide "arm" to chelate to an octahedral Sn atom. The tetradentate $[P_2Se_6]^{4-}$ unit plays a bridging role as in the indium compound. It uses three Se atoms to cap a triangular face of one octahedron [e.g., Se(6), Se(7), and Se(9)] and employs another Se [e.g., Se(10)] to share a corner with a neighboring octahedron (Fig. 2b). There are two sets of Sn–Se distances: the first set of long distances is between Sn and Se(6), Se(7), Se(9), Se(10), with an average distance of 2.75(4) Å, and the second set of short distances is between Sn and Se(1) and Se(5), with an average distance of 2.631(5) Å. The same Sn coordination has been observed in the molecular compounds $A_5Sn(PSe_5)_3$ (A = K, Rb) (2g), with average Sn–Se distances of 2.76(2) Å and 2.66(1) Å for long and short set, respectively. The $[Sn(PSe_5)(P_2Se_6)]_n^{3n-}$ chains are separated by Rb^+ ions located in three different sites. Rb(1) is coordinated by eight Se atoms [range of Rb(1)–Se distances, 3.537(2)–3.881(2) Å; avg. 3.710 Å] and one P atom at 3.785(4) Å, Rb(2) is eight-coordinated [3.613(3)–3.800(2) Å; avg. 3.699 Å], and Rb(3) is eight-coordinated [3.511(3)–3.864(2) Å; avg. 3.694 Å]. Selected distances and angles for $Rb_3Sn(PSe_5)(P_2Se_6)$ are given in Table 5.

Comparison of structures. The most important difference between the two compounds reported here is the oxidation state of the metal center. In the $[Sn(PSe_5)(P_2Se_6)]_n^{3n-}$ chain we find one $[PSe_5]^{3-}$ and one $[P_2Se_6]^{4-}$ equivalent per Sn^{4+} metal center. On the other hand, the $[In_2(PSe_5)_2(P_2Se_6)]_n^{4n-}$ chain contains one $[PSe_5]^{3-}$ and half $[P_2Se_6]^{4-}$ equivalent per metal center for the lower charged In^{3+}. The rare $[PSe_5]^{3-}$ ligand can be derived from the tetrahedral $[PSe_4]^{3-}$ by substitution of an Se_2^{2-} ion for a monoselenide. Known examples of compounds containing this group include $[PPh_4]_2[Fe_2(CO)_4(PSe_5)_2]$ (12), $A_5Sn(PSe_5)_3$ (2g), (A = K, Rb) and $A_6Sn_2Se_4(PSe_5)_2$ (A = Rb, Cs), all of which contain finite molecular anions (2g). In the present study, the

TABLE 4
Selected Distances (Å) and Angles (°) for $K_4In_2(PSe_5)_2(P_2Se_6)$ with Standard Deviations in Parentheses

In(1)–Se(1)	2.757(3)	P(3)–Se(7)	2.209(6)	Se(7)–In(1)–Se(1)	93.18(8)
In(1)–Se(6)	2.746(3)	P(3)–Se(8)	2.164(6)	Se(7)–In(1)–Se(6)	86.55(8)
In(1)–Se(7)	2.799(3)	P(3)–Se(9)	2.184(7)	Se(7)–In(1)–Se(11)	91.25(8)
In(1)–Se(11)	2.828(3)	P(3)–Se(10)	2.243(6)	Se(7)–In(1)–Se(12)	83.12(8)
In(1)–Se(12)	2.789(3)	P(4)–Se(13)	2.262(6)	Se(7)–In(1)–Se(14)	174.48(10)
In(1)–Se(14)	2.742(3)	P(4)–Se(14)	2.223(6)	Se(9)–In(2)–Se(11)	94.31(8)
In(2)–Se(2′)	2.726(3)	P(4)–Se(15)	2.162(6)	Se(9)–In(2)–Se(12)	82.98(8)
In(2)–Se(5′)	2.695(3)	P(4)–Se(16)	2.184(6)	Se(9)–In(2)–Se(16)	171.57(9)
In(2)–Se(9)	2.751(3)			Se(9)–In(2)–Se(2′)	95.90(8)
In(2)–Se(11)	2.789(3)	Se(10)–Se(11)	2.335(3)	Se(9)–In(2)–Se(5′)	89.09(8)
In(2)–Se(12)	2.835(3)	Se(12)–Se(13)	2.341(3)		
In(2)–Se(16)	2.748(3)			Se(1)–P(1)–Se(2)	107.1(2)
				Se(1)–P(1)–Se(3)	116.2(2)
P(1)–Se(1)	2.192(6)	P(1)–P(2)	2.247(7)	Se(1)–P(1)–P(2)	103.8(2)
P(1)–Se(2)	2.241(6)			Se(7)–P(3)–Se(8)	114.2(3)
P(1)–Se(3)	2.134(6)	In(1)–In(2)	4.036(2)	Se(7)–P(3)–Se(9)	114.2(3)
P(2)–Se(4)	2.136(6)			Se(7)–P(3)–Se(10)	107.3(3)
P(2)–Se(5)	2.239(5)				
P(2)–Se(6)	2.193(6)			P(1)–Se(1)–In(1)	97.7(2)
				In(1)–Se(7)–P(3)	103.8(2)
				P(3)–Se(10)–Se(11)	99.8(2)
				Se(10)–Se(11)–In(1)	103.47(10)
				In(1)–Se(11)–In(2)	91.86(8)
				P(3)–Se(10)–Se(11)–In(1)	47.7(2)
				P(3)–Se(10)–Se(11)–In(2)	47.0(2)

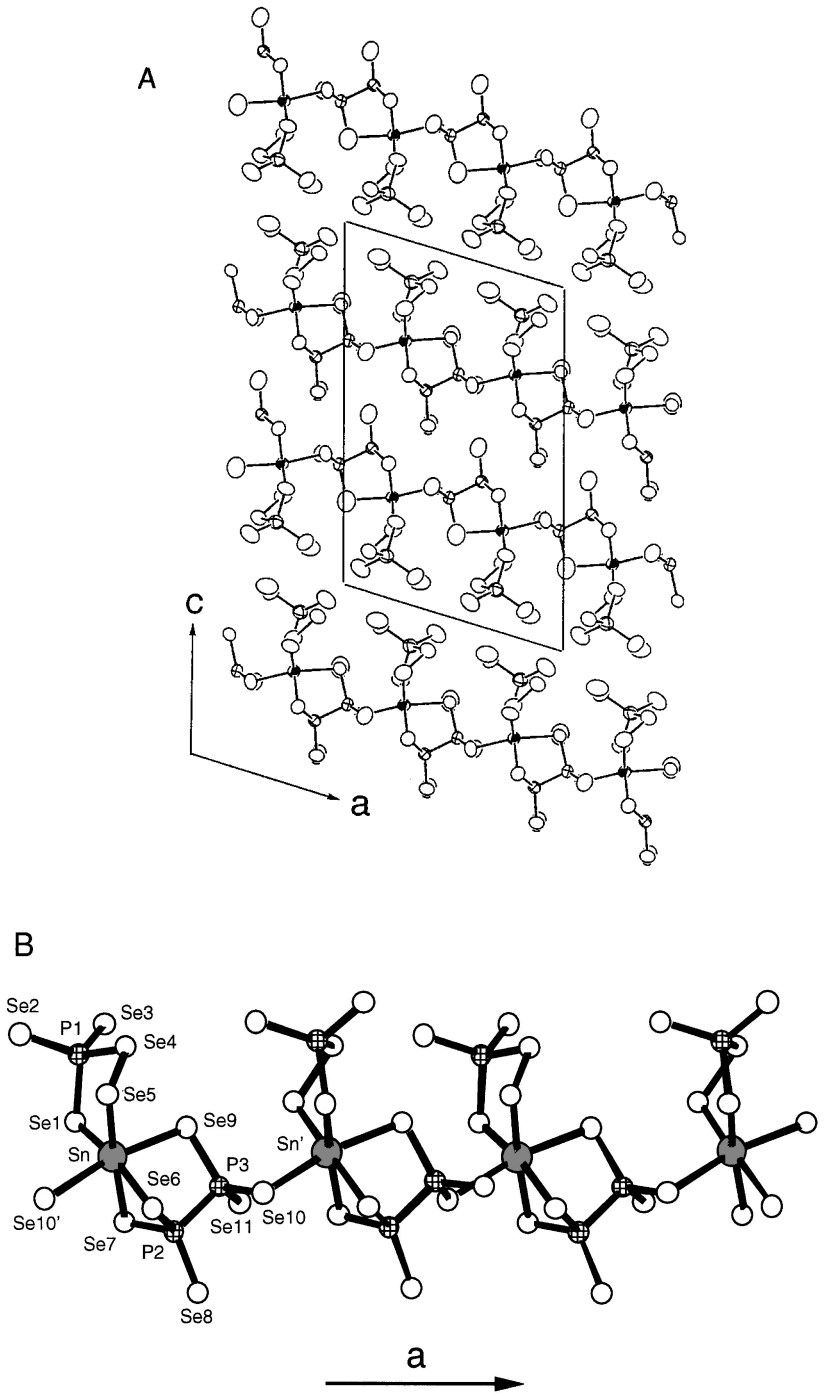

FIG. 2. (A) Unit cell of $Rb_3Sn(PSe_5)(P_2Se_6)$ viewed down the *b*-axis. In the infinite part of the structure, tin is shown as octant shaded ellipses, selenium as open ellipses, and phosphorus as crossed ellipses. The Rb^+ ions located between the chains are shown as open ellipses. (B) An isolated $[Sn(PSe_5)(P_2Se_6)]_n^{3n-}$ chain with labeling.

$[PSe_5]^{3-}$ unit, with a different coordination mode in each case, is not involved in the chain propagation in both compounds. The torsion angle around the Se–Se bond in the $[PSe_5]^{3-}$ unit is quite different between the two compounds. For example, the angle for P(3)–Se(10)–Se(11)–In(2) is 47.0(0)°, whereas for P(1)–Se(4)–Se(5)–Sn the angle is 58.6(1)° (a torsion angle of 63.3(1)° has been observed for $A_5Sn(PSe_5)_3$ (A = K, Rb)[2g]). The $[P_2Se_6]^{4-}$

TABLE 5
Selected Distances (Å) and Angles (°) for $Rb_3Sn(PSe_5)(P_2Se_6)$ with Standard Deviations in Parentheses

Sn–Se(1)	2.634(2)	Se(5)–Sn–Se(1)	96.55(6)
Sn–Se(5)	2.627(2)	Se(5)–Sn–Se(6)	97.48(6)
Sn–Se(6)	2.719(2)	Se(5)–Sn–Se(7)	175.51(6)
Sn–Se(7)	2.779(2)	Se(5)–Sn–Se(9)	89.02(5)
Sn–Se(9)	2.790(2)	Se(5)–Sn–Se(10′)	102.41(6)
Sn–Se(10′)	2.724(2)		
		Se(1)–P(1)–Se(2)	108.6(2)
P(1)–Se(1)	2.244(5)	Se(1)–P(1)–Se(3)	110.1(2)
P(1)–Se(2)	2.163(4)	Se(1)–P(1)–Se(4)	106.4(2)
P(1)–Se(3)	2.137(4)	Se(6)–P(2)–Se(7)	105.4(1)
P(1)–Se(4)	2.290(5)	Se(6)–P(2)–Se(8)	114.8(2)
		Se(6)–P(2)–P(3)	105.7(2)
P(2)–Se(6)	2.218(4)		
P(2)–Se(7)	2.216(4)	Sn–Se(1)–P(1)	104.9(1)
P(2)–Se(8)	2.135(4)	Sn–Se(5)–Se(4)	93.98(7)
P(3)–Se(9)	2.232(4)	Sn–Se(6)–P(2)	81.0(1)
P(3)–Se(10)	2.224(4)	Sn–Se(9)–P(3)	98.5(1)
P(3)–Se(11)	2.131(4)	P(3)–Se(10)–Sn	102.0(1)
Se(4)–Se(5)	2.341(2)	P(1)–Se(4)–Se(5)–Sn	58.6(1)
P(2)–P(3)	2.231(5)		

unit is tetradentate in both frameworks, but it adopts a different coordination mode in each case. Interestingly, in both compounds the $[P_2Se_6]^{4-}$ unit is bridging the fragments to build the one-dimensional structure. The larger ionic radius of the six-coordinate In^{3+} (0.80 Å) (13) compared to six-coordinate Sn^{4+} (0.69 Å) (13) does not appear to have any significant effect other than the longer In–Se distances.

Synthesis, Spectroscopy, and Thermal Analysis

The syntheses of these compounds involve a redox reaction in which the metals are oxidized by polyselenide ions in the $A_x[P_ySe_z]$ flux. The Sn^{4+} or In^{3+} centers are then coordinated by the highly charged $[P_ySe_z]^{n-}$ ligands. Good control of the Lewis basicity of the flux can be achieved by varying the starting composition (3f). In the present experiments the flux was relatively less basic (Lewis), such as to obtain compounds with the $[P_2Se_6]^{4-}$ unit, which contains P^{4+}. Instead, both compounds possess $[P_2Se_6]^{4-}$- and $[PSe_5]^{3-}$-containing P^{4+} and P^{5+} respectively, indicating the presence of complicated Lewis acid-base equilibria.

The optical absorption properties of the compounds were evaluated by examining the solid-state UV/vis diffuse reflectance spectra of the materials (Fig. 3). The spectra suggest that the compounds are semiconductors by revealing the presence of sharp optical gaps. From these spectra, the bandgap, E_g, can be assessed at 2.11 eV for $K_4In_2(PSe_5)_2(P_2Se_6)$ and 1.51 eV for $Rb_3Sn(PSe_5)(P_2Se_6)$.

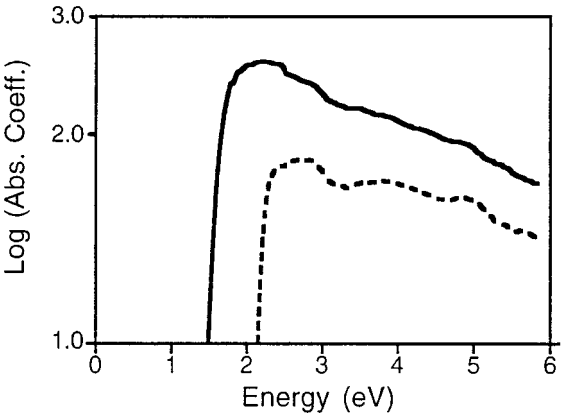

FIG. 3. Solid-state optical absorption spectra of $K_4In_2(PSe_5)_2(P_2Se_6)$ (dashed line) and $Rb_3Sn(PSe_5)(P_2Se_6)$ (solid line).

The far-IR spectrum of $K_4In_2(PSe_5)_2(P_2Se_6)$ displays absorptions at approximately. 486, 469, 451, 427, 304, 225, 184, 150, and 135 cm^{-1}, whereas $Rb_3Sn(PSe_5)(P_2Se_6)$ displays absorptions at approximately, 516, 490, 458, 452, 420, 389, 299, 225, 203, 186, 166, and 144 cm^{-1}. The absorptions above 200 cm^{-1} are assigned to P–Se vibrations of the $[P_2Se_6]^{4-}$ and $[PSe_5]^{3-}$ units, with the characteristic Se–Se vibration appearing at approximately 225 cm^{-1} (2g, 3a). The absorptions below 200 cm^{-1} are probably due to M–Se vibrations (M = In, Sn) (2, 3).

Differential thermal analysis (DTA) data, followed by careful XRD analysis of the residues, show that $Rb_3Sn(PSe_5)(P_2Se_6)$ melts incongruently at 426°C, yielding mainly $SnSe_2$. The DTA of $K_4In_2(PSe_5)_2(P_2Se_6)$ displays more interesting behavior. The first cycle (Fig. 4a) shows a single endothermic peak at about 420°C, but no exothermic peaks appear on cooling. Examination of the residue with XRD analysis reveals only the presence of In_2Se_3. On subsequent heating, an exothermic peak is observed at about 300°C (Fig. 4b), indicating crystallization. Further heating results in the same endothermic peak at about 418°C. If the heating in the above experiment is terminated at 350°C, the XRD pattern of the residue matches that of $K_4In_2(PSe_5)_2(P_2Se_6)$. We attribute this behavior to a phase transformation of $K_4In_2(PSe_5)_2$ (P_2Se_6) to In_2Se_3 and an amorphous glass of nominal composition "$K_4P_4Se_{13}$" at 420°C, according to the reaction

$$K_4In_2(PSe_5)_2(P_2Se_6) \xrightarrow{420°C} In_2Se_3 + \text{“}K_4P_4Se_{13}\text{”}. \quad [1]$$

Upon reheating, In_2Se_3 and "$K_4P_4Se_{13}$" recombine, exothermically, to form the starting compound $K_4In_2(PSe_5)_2$ (P_2Se_6) at 300°C. The decomposition of selenophosphate frameworks to simpler binary compounds and amorphous

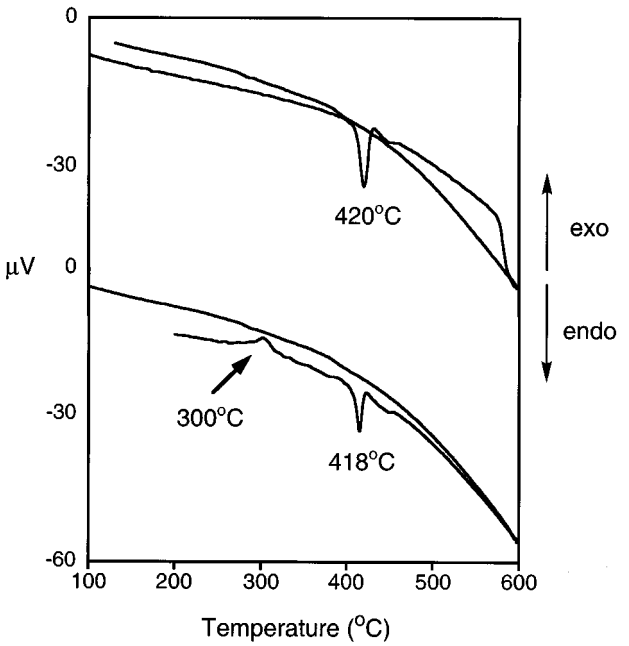

FIG. 4. DTA diagram for $K_4In_2(PSe_5)_2(P_2Se_6)$. (A) First cycle, (B) second cycle.

glass has been observed previously in other compounds (3b, 3e, 4b), but this is the first case in which we observe reversibility of the decomposition reaction on reheating the decomposed byproducts. It is noteworthy that $(Ph_4P)[In(Se_6)_2]$ displays a similar thermal behavior (14).

One of the appealing features of the chalcophosphate flux method is the possibility to obtain different $[P_yQ_z]^{n-}$ groups to coexisting in the same compound. In this type of chemistry, the metal is given the freedom to choose its own ligands suitable for lattice construction. Although we have developed a working knowledge as to which type of $[P_yQ_z]^{n-}$ groups (i.e., P^{4+} or P^{5+}) are likely to be stable in certain flux compositions, the prediction of the exact ligands, especially when two different ones are involved in the same compound, is very difficult. It is hoped that further work, already in progress, will shed some light on the role of the metal center in the complex acid-base equilibria of these reactions.

Supporting information available includes tables of anisotropic thermal parameters of all atoms, interatomic distances and angles, calculated and observed X-ray powder patterns (55 pages).

ACKNOWLEDGMENTS

Financial support from the National Science Foundation DMR-9527347 is gratefully acknowledged. MGK is an A. P. Sloan Foundation and a Camille and Henry Dreyfus Teacher Scholar, 1993–1998. This work made use of the SEM facilities of the Center for Electron Optics at Michigan State University. The authors are grateful to the X-Ray Crystallographic Laboratory of the University of Minnesota and to Victor G. Young Jr. for collecting the single crystal X-Ray data set for $K_4In_2(PSe_5)_2(P_2Se_6)$.

REFERENCES

1. M. G. Kanatzidis, *Curr. Opinion Solid State and Mater. Sci.* **2,** 139 (1997).
2. (a) T. J. McCarthy and M. G. Kanatzidis, *Chem. Mater.* **5,** 1061 (1993); (b) T. J. McCarthy and M. G. Kanatzidis, *J. Chem. Soc., Chem. Commun.* 1089 (1994); (c) T. J. McCarthy, T. Hogan, C. R. Kannewurf, and M. G. Kanatzidis, *Chem. Mater.* **6,** 1072 (1994); (d) T. J. McCarthy and M. G. Kanatzidis, *J. Alloys Comp.* **236,** 70 (1996); (e) K. Chondroudis and M. G. Kanatzidis, Materials Research Society, Fall 1996 meeting, Boston, MA; (f) K. Chondroudis, T. J. McCarthy, and M. G. Kanatzidis, *Inorg. Chem.* **35,** 840 (1996); (g) K. Chondroudis and M. G. Kanatzidis, *J. Chem. Soc., Chem. Commun.* 1371 (1996).
3. (a) T. J. McCarthy and M. G. Kanatzidis, *Inorg. Chem.* **34,** 1257 (1995); (b) K. Chondroudis and M. G. Kanatzidis, *Inorg. Chem.* **34,** 5401 (1995); (c) K. Chondroudis, T. J. McCarthy, and M. G. Kanatzidis, *Inorg. Chem.* **35,** 3451 (1996); (d) K. Chondroudis and M. G. Kanatzidis, *J. Chem. Soc., Chem. Commun.* 401 (1997); (e) K. Chondroudis and M. G. Kanatzidis, *Angew. Chem.* **36,** 1324 (1997); (f) K. Chondroudis, J. A. Hanko, and M. G. Kanatzidis, *Inorg. Chem.* **36,** 2623 (1997); (g) K. Chondroudis, M. G. Kanatzidis, J. Sayettat, S. Jobic, and R. Brec, *Inorg. Chem.*, in press.
4. (a) K. Chondroudis and M. G. Kanatzidis, *C. R. Acad. Sci. Paris, Series B* **322,** 887 (1996); (b) K. Chondroudis and M. G. Kanatzidis, *J. Am. Chem. Soc.* **119,** 2574 (1997).
5. CERIUS^2, Version 1.6, Molecular Simulations Inc., Cambridge, England, 1994.
6. T. J. McCarthy, S.-P. Ngeyi, J.-H. Liao, D. DeGroot, T. Hogan, C. R. Kannewurf, and M. G. Kanatzidis, *Chem. Mater.* **5,** 331 (1993).
7. N. Walker and D. Stuart, *Acta Crystallogr. Sect. A* **39,** 158 (1983).
8. R. H. Blessing, *Acta Crystallogr. Sect. A* **51,** 33 (1995).
9. (a) G. M. Sheldrick, C. Kruger, and R. Doddard, *in* "Crystallographic Computing 3," p. 175. Oxford University Press, Oxford, England, 1985; (b) G. J. Gilmore, *Appl. Cryst.* **17,** 42 (1984).
10. W. Tremel, H. Kleinke, V. Derstroff, and C. Reisner, *J. Alloys Comp.* **219,** 73 (1995).
11. (a) R. Diehl and C. D. Carpentier, *Acta Crystallogr. Sect. B* **34,** 1097 (1978); (b) A. Katty, S. Soled, and A. Wold, *Mater. Res. Bull.* **12,** 663 (1977).
12. J. Zhao, W. T. Pennington, and J. W. Kolis, *J. Chem. Soc., Chem. Commun.* 265 (1992).
13. R. D. Shannon, *Acta Crystallogr. Sect. A* **32,** 751 (1976).
14. S. Dhingra and M. G. Kanatzidis, *Science*, **258,** 1769 (1992).